



**Target Protectors Reveal Dampening and Balancing of Nodal Agonist and Antagonist by miR-430**

Wen-Yee Choi, *et al.*  
*Science* **318**, 271 (2007);  
DOI: 10.1126/science.1147535

***The following resources related to this article are available online at [www.sciencemag.org](http://www.sciencemag.org) (this information is current as of October 15, 2007):***

**Updated information and services**, including high-resolution figures, can be found in the online version of this article at:

<http://www.sciencemag.org/cgi/content/full/318/5848/271>

**Supporting Online Material** can be found at:

<http://www.sciencemag.org/cgi/content/full/1147535/DC1>

This article **cites 20 articles**, 5 of which can be accessed for free:

<http://www.sciencemag.org/cgi/content/full/318/5848/271#otherarticles>

This article has been **cited by** 1 articles hosted by HighWire Press; see:

<http://www.sciencemag.org/cgi/content/full/318/5848/271#otherarticles>

Information about obtaining **reprints** of this article or about obtaining **permission to reproduce this article** in whole or in part can be found at:

<http://www.sciencemag.org/about/permissions.dtl>

teins, but ArLEA1B does not and is itself sensitive to desiccation.

Some LEA proteins have a capacity to associate with and stabilize phospholipid bilayers on dehydration (11, 16, 23). Membrane interaction was assessed with Fourier transform infrared spectroscopy of liposomes dried in the presence of the bdelloid LEA proteins or AavLEA1. The gel-to-liquid crystalline phase-transition temperature ( $T_m$ ) of dried palmitoyl oleoyl phosphatidylcholine (POPC) vesicles ( $59.8^\circ \pm 1.2^\circ\text{C}$ ) was not affected by the presence of ArLEA1A ( $58.2^\circ \pm 1.1^\circ\text{C}$ ) or AavLEA1 ( $61.9^\circ \pm 5.3^\circ\text{C}$ ). However, ArLEA1B significantly decreased  $T_m$  to  $51.8^\circ \pm 2.9^\circ\text{C}$ , which indicates that it interacts with lipids. Further examination of the spectra in the asymmetric phosphate-stretching region revealed a distinct effect of ArLEA1B with a marked shoulder at  $1242\text{ cm}^{-1}$  (Fig. 4). The peaks were resolved into two components attributed to  $\nu\text{P}=\text{Oas}_{\text{free}}$  ( $1262\text{ cm}^{-1}$ ) and  $\nu\text{P}=\text{Oas}$  H-bonded ( $1242\text{ cm}^{-1}$ ) (24), similar to the effect of water and sugar (25). The correlation coefficients for the fitted curves were higher than 0.999. The small bonded P=O population in the absence of protein is because of interlipid charge-pair interactions between P=O and choline groups, whereas the separation of the two P=O populations is probably because ArLEA1B was only in contact with the outer monolayer of the liposomes (26). Clearly, a greater proportion of P=O groups are H-bonded in the presence of ArLEA1B compared with ArLEA1A (42% as opposed to 30%), whereas AavLEA1 has an intermediate value (36%). These results show that ArLEA1B has a stronger propensity to interact with dry phospholipid membranes than ArLEA1A and AavLEA1.

In summary, the bdelloid LEA proteins, encoded by gene copies representing former alleles,

have different structures and functions. These functional differences are likely to be adaptive, because prevention of protein aggregation and protection of cellular membranes are essential for survival of desiccation (10, 27). The presence of complementary activities in a single gene pair of a desiccation-tolerant bdelloid rotifer illustrates the potential for functional diversity resulting from divergence of former alleles. The process of abandoning sexual reproduction and meiosis, and the resulting sequence homogenization of homologous chromosomes, is similar to genome duplication, which is a major evolutionary force (28, 29) that results in orthologous genes evolving relatively independently. Similarly, apomixis could drive evolutionary change by allowing former alleles to diversify in function and may partly explain how bdelloid rotifers have, without genetic exchange, diversified into almost 400 taxonomic species (30, 31).

#### References and Notes

1. D. Mark Welch, M. Meselson, *Science* **288**, 1211 (2000).
2. J. L. Mark Welch, D. B. Mark Welch, M. Meselson, *Proc. Natl. Acad. Sci. U.S.A.* **101**, 1618 (2004).
3. D. B. Mark Welch, M. P. Cummings, D. M. Hillis, M. Meselson, *Proc. Natl. Acad. Sci. U.S.A.* **101**, 1622 (2004).
4. C. W. Birky, *Proc. Natl. Acad. Sci. U.S.A.* **101**, 2651 (2004).
5. M. J. D. White, *Modes of Speciation* (Freeman, San Francisco, 1978).
6. A. Burt, *Evolution* **54**, 337 (2000).
7. M. R. Goddard, H. C. Godfray, A. Burt, *Nature* **434**, 636 (2005).
8. R. Butlin, *Nat. Rev. Genet.* **3**, 311 (2002).
9. C. Ricci, *Hydrobiologia* **387-388**, 321 (1998).
10. A. Tunnacliffe, J. Lapinski, *Philos. Trans. R. Soc. Lond. B Biol. Sci.* **358**, 1755 (2003).
11. A. Tunnacliffe, M. J. Wise, *Naturwissenschaften* **94**, 791 (2007).
12. J. L. Mark Welch, M. Meselson, *Hydrobiologia* **387-388**, 403 (1998).

13. J. A. Browne *et al.*, *Eukaryot. Cell* **3**, 966 (2004).
14. J. Kyte, R. F. Doolittle, *J. Mol. Biol.* **157**, 105 (1982).
15. M. J. Wise, *BMC Bioinform.* **4**, 52 (2003).
16. D. Tolleter *et al.*, *Plant Cell* **19**, 1580 (2007).
17. V. N. Uversky, *Protein Sci.* **11**, 739 (2002).
18. M. T. Sanchez-Ballesta, M. J. Rodrigo, M. T. Lafuente, A. Granell, L. Zacarias, *J. Agric. Food Chem.* **52**, 1950 (2004).
19. J. Grelet *et al.*, *Plant Physiol.* **137**, 157 (2005).
20. J. L. Reyes *et al.*, *Plant Cell Environ.* **28**, 709 (2005).
21. K. Goyal, L. J. Walton, A. Tunnacliffe, *Biochem. J.* **388**, 151 (2005).
22. J. Browne, A. Tunnacliffe, A. Burnell, *Nature* **416**, 38 (2002).
23. P. L. Steponkus, M. Uemura, R. A. Joseph, S. J. Gilmour, M. F. Thomashow, *Proc. Natl. Acad. Sci. U.S.A.* **95**, 14570 (1998).
24. P. T. Wong, H. H. Mantsch, *Chem. Phys. Lipids* **46**, 213 (1988).
25. C. Cacula, D. K. Hincha, *Biophys. J.* **90**, 2831 (2006).
26. D. K. Hincha, E. M. Hellwege, A. G. Heyer, J. H. Crowe, *Eur. J. Biochem.* **267**, 535 (2000).
27. J. H. Crowe, F. A. Hoekstra, L. M. Crowe, *Annu. Rev. Physiol.* **54**, 579 (1992).
28. J. Spring, *Nat. Genet.* **31**, 128 (2002).
29. Y. Van de Peer, *Nat. Rev. Genet.* **5**, 752 (2004).
30. C. W. Birky Jr., C. Wolf, H. Maughan, L. Herberstein, E. Henry, *Hydrobiologia* **546**, 29 (2005).
31. D. Fontaneto *et al.*, *PLoS Biol.* **5**, e87 (2007).
32. We thank J. Mark Welch for advice on FISH and S. Batey for help with CD spectroscopy. Funded by the Biotechnology and Biological Sciences Research Council (519912, BB/D001307/1 and 02/A2/P/08059), the Leverhulme Trust (F/09717/B), the Isaac Newton Trust (6.20), and Integrin Advanced Biosystems Ltd. A.V.P. would like to thank the Deutsche Forschungsgemeinschaft for a travel grant. Sequences are deposited into GenBank with accession numbers EF554863 through EF554866.

#### Supporting Online Material

www.sciencemag.org/cgi/content/full/318/5848/268/DC1  
Materials and Methods  
Figs. S1 and S2  
Table S1  
References and Notes

27 April 2007; accepted 17 August 2007  
10.1126/science.1144363

## Target Protectors Reveal Dampening and Balancing of Nodal Agonist and Antagonist by miR-430

Wen-Yee Choi,<sup>1,2</sup> Antonio J. Giraldez,<sup>1,3\*</sup> Alexander F. Schier<sup>1\*</sup>

MicroRNAs (miRNAs) repress hundreds of target messenger RNAs (mRNAs), but the physiological roles of specific miRNA-mRNA interactions remain largely elusive. We report that zebrafish microRNA-430 (miR-430) dampens and balances the expression of the transforming growth factor- $\beta$  (TGF- $\beta$ ) Nodal agonist *squint* and the TGF- $\beta$  Nodal antagonist *lefty*. To disrupt the interaction of specific miRNA-mRNA pairs, we developed target protector morpholinos complementary to miRNA binding sites in target mRNAs. Protection of *squint* or *lefty* mRNAs from miR-430 resulted in enhanced or reduced Nodal signaling, respectively. Simultaneous protection of *squint* and *lefty* or absence of miR-430 caused an imbalance and reduction in Nodal signaling. These findings establish an approach to analyze the in vivo roles of specific miRNA-mRNA pairs and reveal a requirement for miRNAs in dampening and balancing agonist/antagonist pairs.

MicroRNAs (miRNAs) are small RNA molecules ~22 nucleotides long and function to block the translation and enhance the decay of target mRNAs (1). Recent

studies have uncovered activities of specific miRNA families and have identified hundreds of putative target mRNAs (1–3). However, the physiological roles of specific miRNA-mRNA

pairs are largely unknown (1, 2). To develop a method to disrupt specific miRNA-mRNA pairs, we focused on the zebrafish microRNA-430 (miR-430) family. This miRNA family is highly expressed during early zebrafish development, targets hundreds of mRNAs, and is required for embryonic morphogenesis and clearance of maternal mRNAs (4, 5). Analysis of 3' untranslated regions (3'UTRs) with sites complementary to miR-430 identified *squint* (*sqt*), a member of the Nodal family of transforming growth factor- $\beta$  (TGF- $\beta$ ) signals, and *lft1* and *lft2*, members of the Lefty family of TGF- $\beta$  signals (fig. S1). Nodals are the key regulators of mesoderm induction and left-right axis formation, whereas Leftys act as antagonists of Nodal signaling (6, 7). The balance between Nodals and Leftys

<sup>1</sup>Department of Molecular and Cellular Biology, Harvard University, 16 Divinity Avenue, Cambridge, MA 02138, USA. <sup>2</sup>Developmental Genetics Program, New York University School of Medicine, New York, NY 10016, USA. <sup>3</sup>Department of Genetics, Yale University School of Medicine, New Haven, CT 06510, USA.

\*To whom correspondence should be addressed. E-mail: schier@fas.harvard.edu; antonio.giraldez@yale.edu

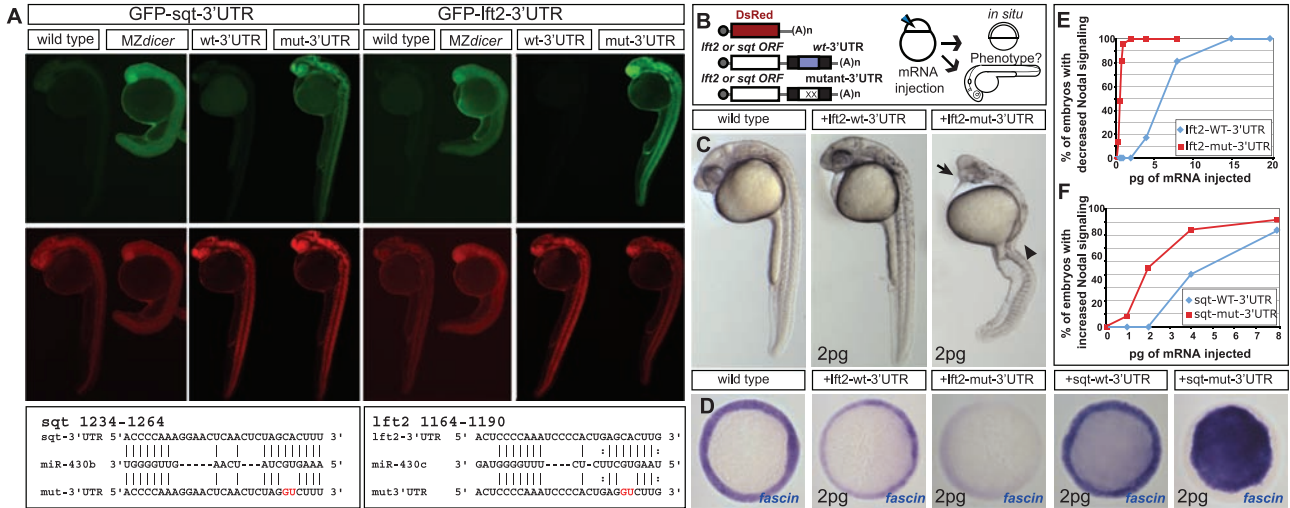
determines the extent of mesendoderm formation (6–8) (fig. S1). Given their potent and concentration-dependent effects, we hypothesized that miR-430 might be required to dampen these signals.

Four lines of evidence indicate that *sqt*, *lft1*, and *lft2* are in vivo targets of miR-430. (i) Reporter mRNAs consisting of the green fluorescence protein (GFP) coding region and full-length *sqt*, *lft1*, or *lft2* 3'UTRs were repressed in the wild type but not in *MZdicer* mutants, which lack all mature miRNAs including miR-430. Derepression of reporter genes was most pro-

nounced for *lft2* and least marked for *lft1*, suggesting that *lft2* is more strongly repressed by miR-430 than *sqt* and *lft1* (Figs. 1A and 2D and figs. S2 and S5). (ii) Mutations of two nucleotides within the miR-430 target site (GCACUU to GGUCUU) abolished repression of reporter mRNAs (Fig. 1A and fig. S2). (iii) Endogenous expression of *sqt*, *lft1*, and *lft2* mRNAs was increased in *MZdicer* mutants (Fig. 3, A and B, and fig. S2). (iv) Misexpression of *sqt*, *lft1*, or *lft2* mRNAs containing mutated miR-430 binding sites (*sqt*<sup>mut-3'UTR</sup>, *lft1*<sup>mut-3'UTR</sup>, *lft2*<sup>mut-3'UTR</sup>)

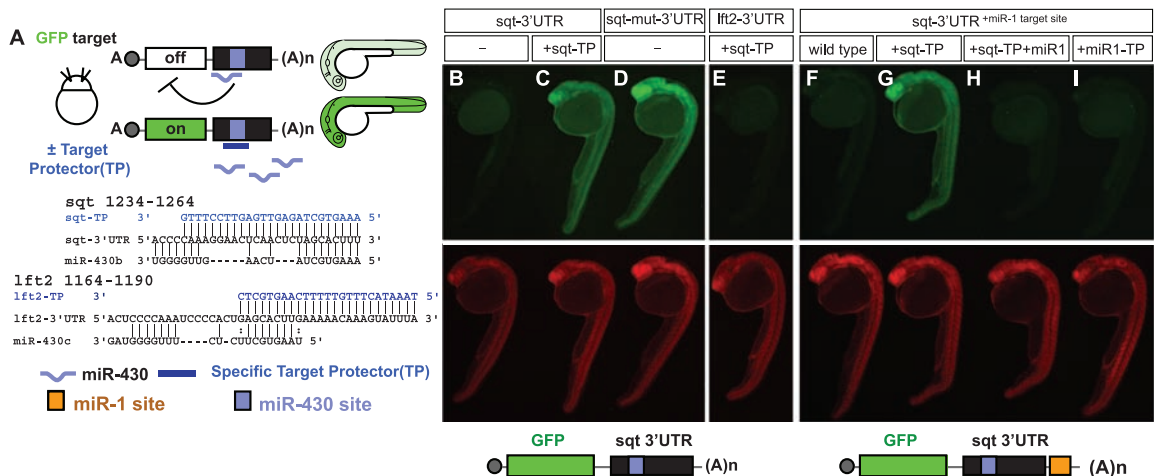
resulted in higher physiological activity (Fig. 1, B to F, and fig. S2). These results indicate that miR-430 represses *sqt*, *lft1*, and *lft2* expression and activity.

To study the physiological role of miR-430/*sqt* and miR-430/*lft2* interactions, we developed a method to disrupt the interaction of miRNAs with target mRNAs. RNA-binding morpholino antisense oligonucleotides are commonly used in zebrafish to block the translation or splicing of target RNAs (9–11). We reasoned that morpholinos overlapping with miRNA target sites might inter-



uninjected controls, whereas injection of 2 pg of *lft2*<sup>mut-3'UTR</sup> mRNA causes cyclopia (arrow) and loss of trunk mesoderm (arrowhead), hallmarks of reduced Nodal signaling. (D) Physiological activity of *sqt* or *lft2* mRNA assessed by *fascin* (*fas*) induction, a marker for Nodal signaling activity. *lft2*<sup>mut-3'UTR</sup> mRNA (2 pg) causes a stronger decrease in *fas* induction than wild-type *lft2*. *sqt*<sup>mut-3'UTR</sup> mRNA (2 pg) leads to greater ectopic induction of *fas* than wild-type *sqt*. (E) Percentage of embryos with decreased Nodal signaling (cyclopia and loss of trunk mesoderm) at increasing concentrations of wild-type *lft2* or *lft2*<sup>mut-3'UTR</sup> mRNA. (F) Percentage of embryos with increased Nodal signaling (ectopic *gsc* induction covering >50% of the animal pole) at increasing concentrations of wild-type *sqt* or *sqt*<sup>mut-3'UTR</sup> mRNA.

**Fig. 2. miRNA target protectors (TPs) interfere with specific miRNA-mRNA interactions.** (A) Experimental approach. Target protectors are co-injected with GFP-reporters (green) into wild-type embryos and prevent miR-430-induced target repression. Predicted pairings of *sqt*-TP<sup>miR-430</sup> and *lft2*-TP<sup>miR-430</sup> to *sqt* and *lft2* 3'UTRs are shown. DsRed mRNA (red) is injected as a control. (B) Wild-type reporter is repressed in wild-type embryos. (C and D) Co-injection of *sqt*-TP<sup>miR-430</sup> or mutation of miR-430 target site prevents GFP repression. (E) *sqt*-TP<sup>miR-430</sup> does not affect repression of *lft2*-GFP reporter. (F) *sqt*-GFP reporter with introduced miR-1 target site is repressed in wild-type embryos. miR-1 is not expressed during early



zebrafish embryogenesis. (G) *sqt*-TP<sup>miR-430</sup> prevents GFP repression in the absence of miR-1. (H) *sqt*-TP<sup>miR-430</sup> does not interfere with activity of injected miR-1. (I) *sqt*-TP<sup>miR-1</sup> does not interfere with miR-430 activity.

fer with miRNA-mRNA interactions, thus protecting the target from the miRNA (target protector, TP) (Fig. 2A). Specificity would be attained by the sequences unique to the 3'UTR. To test this strategy, we analyzed the effect of morpholinos complementary to the region of the miR-430 target sites in the *sqt* or *lft2* 3'UTRs. Four lines of evidence indicate that TPs interfere with miR-430-mediated repression of specific 3'UTRs. (i) Injection of *sqt*-TP<sup>miR-430</sup> blocked miR-430-induced repression of the *sqt*-GFP reporter (Fig. 2, B to D, and fig. S3). (ii) *sqt*-TP<sup>miR-430</sup> did not

block repression of the *lft2*-GFP reporter, suggesting that TPs do not induce cross-protection (Fig. 2E). (iii) Control morpholinos complementary to other regions of the *sqt* 3'UTR did not prevent *sqt*-GFP repression by miR-430 (fig. S4). (iv) Injection of *sqt*-TPs into *MZdicer* mutants did not affect the levels of *sqt*-GFP reporter or *sqt* gene expression, suggesting that TPs do not cause nonspecific stabilization of mRNAs (Fig. 3A and fig. S5). Corresponding results were obtained with *lft2*-TP<sup>miR-430</sup> (Fig. 3B and figs. S2 to S5). To test whether TPs specifically block the interaction with

one target site without affecting the interaction with other target sites in the same 3'UTR, we placed a miR-1 target site into the *sqt*-GFP reporter (Fig. 2, F to I). Protection of the miR-430 target site did not prevent miR-1-mediated GFP repression (Fig. 2H), and protection of the miR-1 target site did not interfere with miR-430-mediated repression (Fig. 2I). Taken together, these results indicate that target protection provides a powerful *in vivo* method to specifically investigate the role of individual miRNA-mRNA target site interactions.

To determine the role of miR-430 repression of *sqt*, we analyzed *sqt*-TP<sup>miR-430</sup>-injected embryos. Similar to *MZdicer* mutants, *sqt* expression was elevated (Fig. 3A). Protection of *sqt* increased the induction of mesodermal marker genes such as *gooseoid* (*gsc*), indicative of higher Nodal signaling during blastula stages (6, 8, 12) (Figs. 3C and 4B and fig. S6). The increased *gsc* induction resulted from the protection of zygotically transcribed but not maternally loaded *sqt* (fig. S7). Ectopic *gsc* induction in *sqt*-TP<sup>miR-430</sup>-injected embryos was suppressed by a morpholino blocking *sqt* translation, indicating that *sqt*-TP<sup>miR-430</sup> specifically increased *sqt* activity (Fig. 3C and fig. S6). To quantify the effects of increased Nodal signaling, we analyzed the number of *sox17*-expressing endoderm progenitors and dorsal forerunner cells during gastrulation (6, 8). Forerunner cells are induced by Nodal signaling at the dorsal margin and form Kupffer's vesicle, an embryonic organ that functions during left-right axis formation (8, 13). Cell counting revealed an increase in the number of endodermal and forerunner cells in *sqt*-TP<sup>miR-430</sup> embryos (Fig. 4, C to E). These results suggest that miR-430 can dampen Nodal signaling by repressing *sqt*.

**Fig. 3.** Target protection results in increased *sqt* and *lft2* expression and activity. (A) *sqt*-TP<sup>miR-430</sup> injection results in elevated *sqt* expression, similar to the finding in *MZdicer* mutants. *sqt*-TP<sup>miR-430</sup> does not increase *sqt* expression in *MZdicer*. (B) *lft2*-TP<sup>miR-430</sup> injection results in elevated *lft2* expression, similar to the finding in *MZdicer* mutants. *lft2*-TP<sup>miR-430</sup> does not increase *lft2* expression in *MZdicer*. (C) *sqt*-TP<sup>miR-430</sup>-injected embryos exhibit increased *gsc* expression (arrowheads) that is suppressed by co-injection of a *sqt*-AUG morpholino. (D) *lft2*-TP<sup>miR-430</sup>-injected embryos display cyclopia (arrowheads) that is suppressed by co-injection of a *lft2*-AUG morpholino.

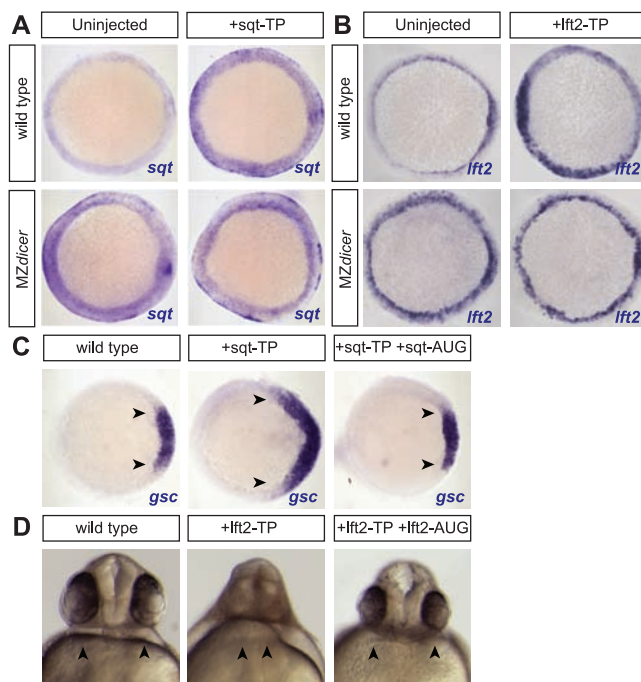
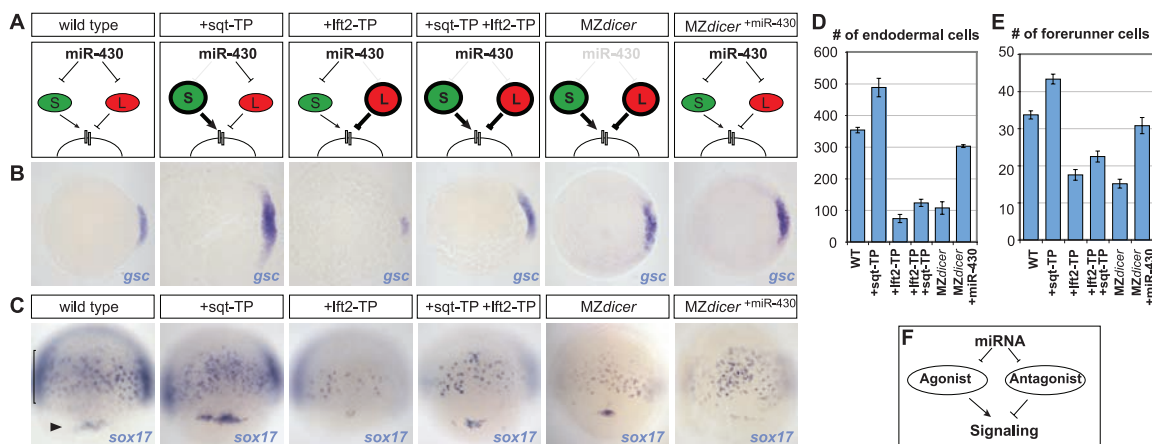


**Fig. 4.** miR-430 maintains the balance between *sqt* and *lft2*. (A) Schematics of miR-430 regulation of *sqt* (S) and *lft2* (L) in wild-type, wild-type + *sqt*-TP<sup>miR-430</sup>, wild-type + *lft2*-TP<sup>miR-430</sup>, wild-type + *sqt*-TP<sup>miR-430</sup> + *lft2*-TP<sup>miR-430</sup>, *MZdicer*, and *MZdicer*<sup>+miR-430</sup> embryos. Removal of miR-430 regulation in each case results in increased *sqt* and/or *lft2* expression. (B) *gsc* expression is increased in *sqt*-TP<sup>miR-430</sup>-injected embryos and decreased in *lft2*-TP<sup>miR-430</sup>-injected embryos. *gsc* induction is similar in wild-type, wild-type + *sqt*-TP<sup>miR-430</sup> + *lft2*-TP<sup>miR-430</sup>, *MZdicer*, and *MZdicer*<sup>+miR-430</sup> embryos at 50% epiboly. (C) *sox17* expression is reduced in wild-type + *sqt*-TP<sup>miR-430</sup> + *lft2*-TP<sup>miR-430</sup> and *MZdicer* embryos as compared to uninjected wild types at 75% epiboly. *sox17* labels endodermal cells (bracket) and forerunner cells (arrowhead). (D) Quantification of *sox17*-expressing endodermal cells ( $n = 5$  to 10 embryos for each genotype per injection). (E) Quantification of *sox17*-expressing forerunner cells ( $n = 12$  to 35 embryos for each genotype per



injection). (D and E) Endodermal and forerunner cell numbers vary from embryo to embryo. Bars represent mean  $\pm$  SEM, which are significantly different between wild-type and wild-type + *sqt*-TP<sup>miR-430</sup> ( $P < 0.0005$  by two-tailed Student's *t* test), wild-type and wild-type + *lft2*-TP<sup>miR-430</sup> ( $P < 10^{-12}$ ), wild-type and wild-type + *sqt*-TP<sup>miR-430</sup> + *lft2*-TP<sup>miR-430</sup> ( $P < 10^{-7}$ ), wild-type and *MZdicer* ( $P < 10^{-8}$ ), wild-type + *lft2*-TP<sup>miR-430</sup> and wild-type + *sqt*-TP<sup>miR-430</sup> + *lft2*-TP<sup>miR-430</sup> ( $P < 0.02$ ), and *MZdicer* and *MZdicer*<sup>+miR-430</sup> ( $P < 10^{-5}$ ) embryos. (F) Model for miRNA-mediated balancing of an agonist and an antagonist.

To determine the *in vivo* role of miR-430 repression of *lft*, we focused on *lft2* because the repression of *lft2* by miR-430 was more pronounced than it was for *lft1* (Fig. 1A and fig. S2). *lft2* target protection resulted in elevated *lft2* expression, similar to the finding in *MZdicer* mutants (Fig. 3B). *lft2*-TP<sup>miR-430</sup>-injected embryos displayed cyclopia, reduced *gsc* expression (Figs. 3D and 4B and fig. S6) (6, 8, 12), and fewer *sox17*-expressing endodermal and fore-runner cells (Fig. 4, C to E). These results indicate that miR-430 can enhance Nodal signaling by dampening *lft2*.

To determine the role of miR-430 in simultaneously dampening both *sqt* and *lft2*, we co-injected *sqt*-TP<sup>miR-430</sup> and *lft2*-TP<sup>miR-430</sup>. The induction of *gsc* was not strongly affected in *sqt/lft2*-TP<sup>miR-430</sup> embryos and *MZdicer* mutants (Fig. 4B), but the expression of *sox17* revealed a reduced number of endodermal and dorsal forerunner cells in *sqt/lft2*-TP<sup>miR-430</sup> embryos and *MZdicer* mutants (Fig. 4, C to E). These results indicate that loss of miR-430 regulation leads to an imbalance of *sqt* and *lft* inputs and reduces some outputs of Nodal signaling.

Our study of miR-430 and Nodal signaling provides two major insights. First, the regulation of *sqt* and *lft2* by miR-430 identifies a role for miRNAs as dampeners and balancers of agonist/antagonist pairs and reveals a previously unknown regulatory layer of Nodal signaling (Fig. 4, A and F, and fig. S1). miR-430 reduces the absolute levels of *sqt* and *lft2* expression (dampening) and regulates their relative levels to achieve optimal activity of the Nodal pathway (balancing). The protection of *sqt* and *lft2* from miR-430 does not appear to lead to major phenotypic changes during blastula stages (*gsc* expression) but reduces Nodal signaling during gastrulation (*sox17* expression). Because Nodal and Lefty signals have complex regulatory interactions (6, 7), multiple mechanisms might contribute to this temporal difference. For example, stronger de-repression (Figs. 1A and 3, A and B) and longer persistence of *lft2* after loss of miR-430 regulation could inhibit *Sqt* and the related Nodal signal Cyclops during gastrulation (6, 8, 12). The regulation of Nodal signaling by miR-430 is likely to be conserved, because miR-430 is found in other vertebrates (miR-302, miR-372, and miR-519) and predicted miR-430 target sites are present in other *Nodal* and *Lefty* genes (fig. S1) (4). More generally, our results reveal a regulatory interaction in which a repressor (miR-430) dampens the expression of both an agonist (*sqt*) and an antagonist (*lft*) (Fig. 4, A and F, and fig. S1). Dampening might not only allow balancing of counteracting inputs but also add robustness (14–18). For example, our overexpression experiments show that the embryo can tolerate increased expression of miR-430-regulated *sqt* or *lft* mRNA, whereas loss of miR-430-mediated regulation leads to gain-of-function phenotypes (Fig. 1C and fig. S2). miRNA-mediated balancing of agonist/antagonist pairs might also contribute to the evolution of phenotypic changes.

The short region of sequence complementarity required for the recognition of miRNA target sites allows for the rapid acquisition, loss, or modulation of miRNA-mRNA target interactions (19–21). Our results raise the possibility that target sequence variations could change the balance of agonist/antagonist expression and induce phenotypic changes such as the expansion or reduction of progenitor fields.

Second, our study introduces a method to test the role of specific miRNA-mRNA pairs *in vivo* (fig. S8). Thousands of miRNA-mRNA interactions have been predicted, but less than a dozen have been shown to have an *in vivo* function (2, 3). The sequence-selectivity of morpholino target protectors makes them excellent agents to disrupt specific miRNA-mRNA interactions. Other antisense oligonucleotides and small molecules that bind to miRNA target sites or their vicinities are also likely to serve as target protectors. Target protectors not only uncover the physiological role of miRNA-mRNA interactions, but also illustrate how miRNA phenotypes are a composite created by up-regulation of multiple targets (fig. S8). Additionally, target protectors might serve as therapeutic agents (fig. S8). More than 30% of all human genes are thought to be miRNA targets (1–3). By blocking the interaction of specific miRNA-mRNA pairs through the use of target protectors, the translation and stability of particular mRNAs could be increased and result in the suppression of hypomorphic mutations or the up-regulation of beneficial gene products such as tumor suppressors or peptide hormones (fig. S8).

#### References and Notes

1. N. Bushati, S. M. Cohen, *Annu. Rev. Cell Dev. Biol.* 10.1146/annurev.cellbio.23.090506.123406 (2007).

2. W. P. Kloosterman, R. H. Plasterk, *Dev. Cell* 11, 441 (2006).
3. N. Rajewsky, *Nat. Genet.* 38 (suppl.), 58 (2006).
4. A. J. Giraldez *et al.*, *Science* 308, 833 (2005).
5. A. J. Giraldez *et al.*, *Science* 312, 75 (2006).
6. A. F. Schier, *Annu. Rev. Cell Dev. Biol.* 19, 589 (2003).
7. M. M. Shen, *Development* 134, 1023 (2007).
8. A. F. Schier, W. S. Talbot, *Annu. Rev. Genet.* 39, 561 (2005).
9. J. Summerton, *Biochim. Biophys. Acta* 1489, 141 (1999).
10. A. Nasevicius, S. C. Ekker, *Nat. Genet.* 26, 216 (2000).
11. B. W. Draper, P. A. Morcos, C. B. Kimmel, *Genesis* 30, 154 (2001).
12. B. Feldman *et al.*, *Nature* 395, 181 (1998).
13. J. J. Essner, J. D. Amack, M. K. Nyholm, E. B. Harris, H. J. Yost, *Development* 132, 1247 (2005).
14. D. P. Bartel, C. Z. Chen, *Nat. Rev. Genet.* 5, 396 (2004).
15. E. Hornstein, N. Shomron, *Nat. Genet.* 38 (suppl.), S20 (2006).
16. A. Becksei, B. B. Kaufmann, A. van Oudenaarden, *Nat. Genet.* 37, 937 (2005).
17. E. M. Ozbudak, M. Thattai, I. Kurtser, A. D. Grossman, A. van Oudenaarden, *Nat. Genet.* 31, 69 (2002).
18. J. M. Raser, E. K. O'Shea, *Science* 309, 2010 (2005).
19. K. Chen, N. Rajewsky, *Nat. Rev. Genet.* 8, 93 (2007).
20. K. Chen, N. Rajewsky, *Nat. Genet.* 38, 1452 (2006).
21. A. Clop *et al.*, *Nat. Genet.* 38, 813 (2006).
22. We thank S. Mango, D. Prober, J. Rihel, C. Stahlhut, A. Staton, and W. Talbot for helpful comments on the manuscript. A.J.G. was supported by European Molecular Biology Organization and Human Frontier Science Program fellowships. This research was also supported by grants from the NIH.

#### Supporting Online Material

www.sciencemag.org/cgi/content/full/1147535/DC1

Materials and Methods

Figs. S1 to S8

References

9 July 2007; accepted 21 August 2007

Published online 30 August 2007;

10.1126/science.1147535

Include this information when citing this paper.

## PKA Type II $\alpha$ Holoenzyme Reveals a Combinatorial Strategy for Isoform Diversity

Jian Wu,<sup>1</sup> Simon H. J. Brown,<sup>1</sup> Sventja von Daake,<sup>1</sup> Susan S. Taylor<sup>1,2\*</sup>

The catalytic (C) subunit of cyclic adenosine monophosphate (cAMP)-dependent protein kinase (PKA) is inhibited by two classes of regulatory subunits, RI and RII. The RII subunits are substrates as well as inhibitors and do not require adenosine triphosphate (ATP) to form holoenzyme, which distinguishes them from RI subunits. To understand the molecular basis for isoform diversity, we solved the crystal structure of an RII $\alpha$  holoenzyme and compared it to the RI $\alpha$  holoenzyme. Unphosphorylated RII $\alpha$ (90–400), a deletion mutant, undergoes major conformational changes as both of the cAMP-binding domains wrap around the C subunit's large lobe. The hallmark of this conformational reorganization is the helix switch in domain A. The C subunit is in an open conformation, and its carboxyl-terminal tail is disordered. This structure demonstrates the conserved and isoform-specific features of RI and RII and the importance of ATP, and also provides a new paradigm for designing isoform-specific activators or antagonists for PKA.

Cyclic adenosine monophosphate (cAMP) is a universal signal for environmental stress. In mammalian cells, major recep-

tors for cAMP are the regulatory (R) subunits of cAMP-dependent protein kinase (PKA) (1, 2). All R subunits share the same domain organiza-